Biochimica et Biophysica Acta, 1148 (1993) 152–156

BBAMEM 75975

The distribution of intracellular calcium chelator (fura-2) in a population of intact human red cells

Virgilio L. Lew [a,b], Zipora Etzion [a,b], Robert M. Bookchin [a,b], Rui daCosta [c], Heikki Väänänen [c], Massimo Sassaroli [c] and Josef Eisinger [b]

[a] *Physiological Laboratory, Cambridge (UK),* [b] *Albert Einstein College of Medicine, New York, NY (USA) and* [c] *Department of Physiology and Biophysics, Mount Sinai School of Medicine, New York, NY (USA)*

(Received 15 October 1992)

Key words: Fura-2; Cytometry; Calcium chelator; (Erythrocyte)

Using quantitative fluorescence microscopy of red cells loaded non-disruptively with 1–2.5 mmol/l cells of fura-2, we examined the distribution of the incorporated free chelator among and within individual cells. Cytoplasmic hemoglobin quenched the effective fluorescence yield of fura-2 by a factor of about 100. All red cells were found to fluoresce upon excitation at 380 nm, and the fluorescence intensities they emitted at 510 nm were approximately ±20% about the mean intensity, indicating a fairly uniform distribution of incorporated chelator among the cells. Red cells loaded with these high levels of fura-2 retained their biconcave shape, and a comparison between their transmission images at 415 nm and their fura-2 fluorescence images suggests that the concentration of fura-2 was also uniform throughout the cytosol. These results validate assumptions made in earlier experiments with non-fluorescent incorporated Ca^{2+} chelators, and demonstrate the feasibility of fura-2 and Ca^{2+} imaging of intact red cells, despite considerable quenching of probe fluorescence by hemoglobin.

Introduction

The non-fluorescent Ca^{2+} chelator benz-2, with a K_d for Ca^{2+} of about 50 nM, was a crucial tool for the characterization of the physiological $[Ca^{2+}]_i$ level, pump-leak turnover and Ca^{2+}-pump kinetics in intact red cells [1]. Incorporation of benz-2 increases the cytosolic Ca^{2+} binding pool allowing precise measurements of changes in $[Ca^{2+}]_i$ from ^{45}Ca tracer distributions, over the physiological range of 10–30 nM and as low as 1–2 nM $[Ca^{2+}]_i$ [1]. Thus far, there are no fluorescent Ca^{2+} indicators available with a K_d as low as that of benz-2, i.e., low enough for single cell Ca^{2+} imaging in that $[Ca^{2+}]_i$ range. Furthermore, for chelators with fluorescent yields similar to those of fura-2, quenching of the fluorescent signal by hemoglobin would raise the required chelator loads to levels much higher than those sufficient in studies with benz-2. Despite these problems, the foreseeable advantages of single cell Ca^{2+} imaging for answering specific questions about the pathophysiology of red cell Ca^{2+} [2–6] justify preparatory studies with available fluorescence probes such as fura-2.

A major question in studies with chelator-loaded red cell populations concerns the uniformity of chelator concentration among cells. If the distribution of chelator in the cell population were very uneven, the true distribution of cell $[Ca^T]_i$ would be broader than that assumed with uniform chelator levels, and the interpretation of results obtained using such methods would have to be substantially revised. There is indirect evidence suggesting that free chelator is released in all the cells of a sample incubated with the acetoxy methyl derivative, and that its distribution may be fairly uniform. Tsien [7] demonstrated that intact red cells loaded with benz-2 all exhibited a characteristic delay (as compared with benz-2-free controls) in the activation of Ca^{2+}-sensitive ^{86}Rb fluxes after exposure to ionophore A23187 and external Ca^{2+}. This indicated that all cells had incorporated chelator. Findings by Lew et al. [1], that the initial Ca^{2+} influx into benz-2-loaded red cells with normal ATP was similar to that into ATP-depleted cells with or without incorporated chelator, indicated that benz-2 did not increase the passive Ca^{2+} permeability of the red cell membrane and that its distribution could not be grossly uneven. However, the distribution of Ca^{2+} chelators incorporated into intact red cells has never been measured directly. The present fluorescence imaging experiments investigate the distribution of incorporated fura-2 levels among the red cells and also its spatial distribution within individual cells.

Correspondence to: V.L. Lew, Physiological Laboratory, Cambridge University, Downing Street, Cambridge CB2 3EG, UK.

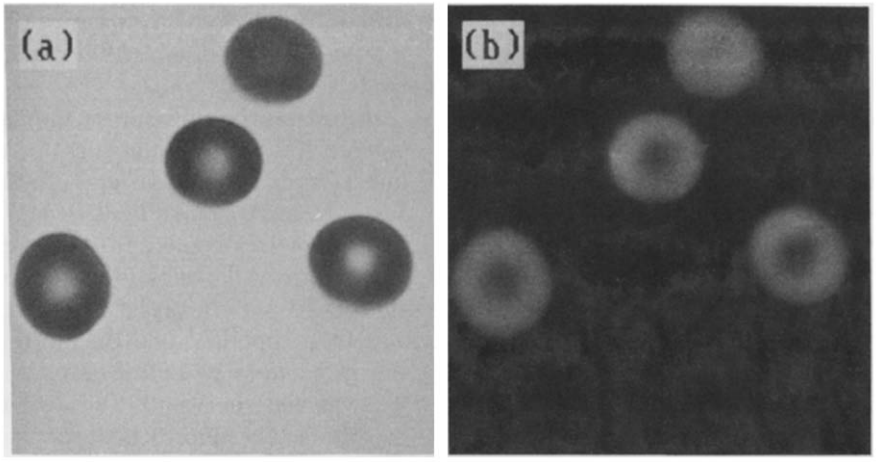

Fig. 1. Portions of a pair of (a) 415 nm transmission and (b) fura-2 fluorescence images of fura-2-loaded red cells, acquired with the 100× objective under the conditions described in the text.

Materials and Methods

Fura-2 loading of red cells. The fura-2-loading procedure was similar to that described before for benz-2 [1,8]. Heparinized blood was obtained from normal donors and the red cells were washed three times in solution A containing (in mM): KCl, 80; NaCl, 70; $MgCl_2$, 0.15; Na-Hepes (pH 7.4–7.5 at 37°C), 10 and Na-EGTA, 0.1. The buffy coat was removed after each wash. The cells (10–50 μl) were resuspended at 1–5% hematocrit at room temperature in solution B, which is solution A supplemented with 10 mM inosine as metabolic substrate, and 5 mM pyruvate to bypass the metabolic block generated by the release of formaldehyde during chelator incorporation and thus prevent ATP depletion [9–11]. The acetoxy methyl derivative of fura-2 (fura-2-AM, Sigma, St. Louis, MO, USA) was added to this suspension from 5 or 50 mM stock solutions in DMSO under vigorous stirring, continued for about 1 min. The suspension was then incubated for 90–120 min at 37°C with intermittent mixing. Finally, the cells were centrifuged, washed once in solution B and kept loosely packed at approx. 50–70% hematocrit and approx. 4°C. For observation and imaging, aliquots of this suspension were diluted to 10–40% hematocrit in solution B containing, in addition, bovine serum albumin (BSA), 1 g/dl.

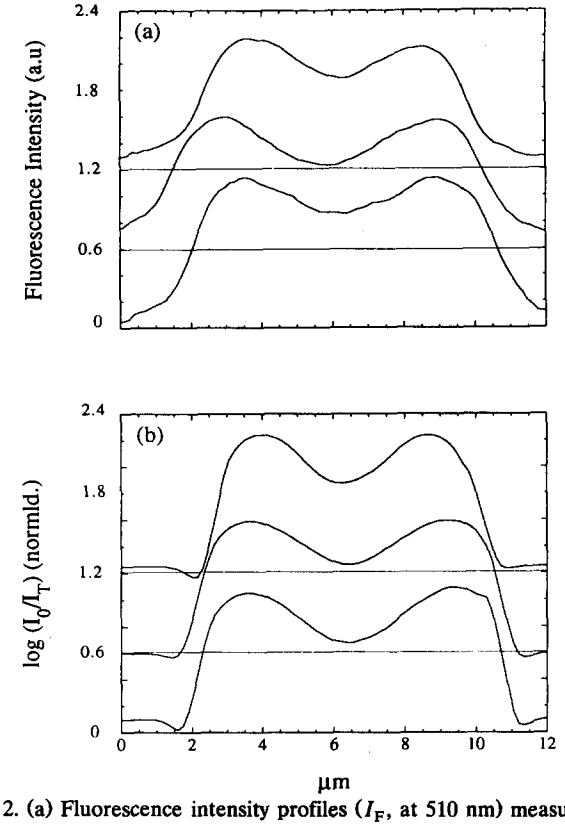

Fig. 2. (a) Fluorescence intensity profiles (I_F, at 510 nm) measured along diameters of the fluorescence images of three typical fura-2-loaded red cells. (b) Log (I_o/I_T) profiles measured along the same diameters, with I_T and I_o derived from the transmission images (at 415 nm) of the same three cells. As discussed in the text, the profiles shown in (a) and (b) are expected to be approximately proportional to each other (cf., Eqns. 1 and 3). 'a.u.', arbitrary units; 'normald.', normalized.

Preliminary experiments indicated that satisfactory imaging could be obtained by exposing the cells to 1 to 2.5 mmol/l cells of fura-2-AM. These loads were large enough to provide intense fluorescence images with the short exposures needed to avoid blurring due to slight mobility of the cells settled at the bottom of the viewing chamber. *

To estimate the extent of quenching of fura-2 incorporated in the red cell cytoplasm, we compared its

* Trials had indicated that red cells attached to coated surfaces (polylysine, agar casting) for immobilization lost their normal biconcave shape and a variable fraction lysed, raising doubts about the functional integrity of the remaining cells. Other trials showed that when the red cells were resuspended in autologous plasma, they formed rouleaux which interfered with single cell imaging.

fluorescence yields with that of fura-2 dissolved in solution A. When a special specimen chamber with a 12 μm space between cover glasses was filled with 0.1 and 1.0 mM solutions of fura-2, the slab-shaped volumes of solution imaged by the CCD camera showed an average fluorescence yield (in electrons/s per pixel per μm thickness) of 250 and 2700, respectively. By comparison, fura-2-loaded red cells had an average yield of 50 e^-/s per pixel per about 1 μm cell thickness. Since the cytoplasmic fura-2 was approx. 2 mM, this indicates that the fluorescence of fura-2 is quenched about 100-fold within the red cell.

Image acquisition and analysis. Images were obtained with an inverted fluorescence microscope (Axiovert, C. Zeiss, Thornwood, NY, USA), using either a Neofluar 40 ×, 1.3 NA or a Neofluar 100 ×, 1.3 NA Zeiss objective. The fura-2-loaded cell suspensions were delivered into a plastic cylinder 5 mm high and 5 mm in diameter attached to a standard (0.17 mm) cover glass. After the cells settled to the bottom of this chamber, each field was imaged in two modes: in the transmitted light mode at 415 nm (the heme Soret band), and in the epi-illuminated fluorescence mode at 510 nm, upon excitation at 340 or 380 nm. Interference filters with a band pass of 10 to 20 nm provided the requisite excitation and emission wavelengths, and a dichroic mirror reflective above 400 nm was used to separate the excitation from the emission light (Omega Optical, Brattleboro, VT, USA). The images were acquired by a cooled, slow-scan CCD camera (Astromed, Cambridge, UK) with exposure times of 0.15 and 5 s for the transmission and fluorescence images, respectively.

After background subtraction and 'flat-fielding' to correct for heterogeneity in the excitation light, the images were analyzed using TCL-Image software (TNO Institute of Applied Physics, Delft, Netherlands) on a Macintosh IIcx computer. After rescaling to 8-bits accuracy, the cell edges in the absorption images were sharpened and an object mask was created; the mask was then superimposed on the fluorescence image of the same field to define the perimeter of each cell, with partial or 'small' cells excluded by a suitable algorithm. The fluorescence intensities recorded by the pixels within each cell image were integrated to obtain the total fluorescence emitted by each cell, and from these data, the histogram showing the frequency distribution of total cell fluorescence was constructed. Details of the image acquisition, storage, processing and analysis are given elsewhere [12,13].

Results and Discussion

In two control studies it was shown that (i), no detectable fluorescence was elicited from fura-2-free cells under similar conditions and (ii), when fura-2-loaded cells were exposed to external Ca^{2+} and the non-fluorescent Ca^{2+} ionophore ionomycin, the emission intensity ratio for excitation at 340 and 380 nm, respectively, increased. For example, when $[Ca^{2+}]_o$ was

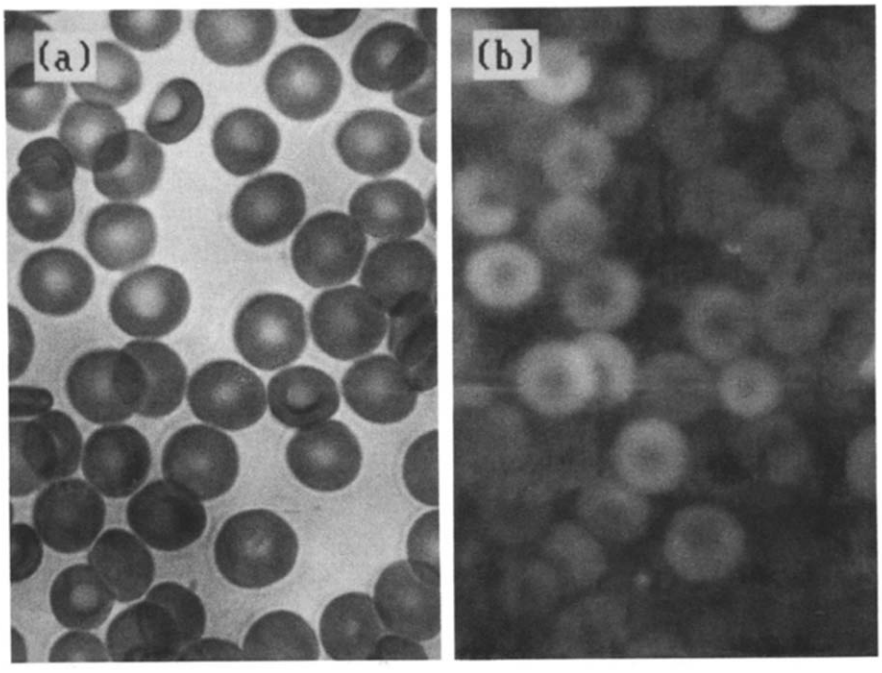

Fig. 3. A pair of (a) transmission and (b) fluorescence images of fura-2-loaded red cells. Several similar fields, diluted approx. five-fold to reduce cell overlap, were analyzed to obtain the distribution histogram of cell fluorescence intensities shown in Fig. 4. The total intensity emitted by each cell is reflected accurately in the histogram obtained from the digitized images (see Materials and Methods), and not in the visual appearance of screen photographs such as this, reproduced with unavoidable enhanced contrast, for illustration purposes only.

raised from approx. 0 to 270 μM, the 340/380 intensity ratio increased from 0.5 to 3.5. These results indicate that intrinsic fluorescence does not contribute to the fluorescence images shown in Fig. 1b and that the intracellular fura-2 responded to the Ca^{2+} level as expected for the free chelator [14]. It should be noted, however, that the intensity of the excitation light was greater at 380 nm than at 340 nm, largely because of the reduced efficiency of the microscope optics at the shorter wavelength.

Fig. 1a and b shows paired transmission and fluorescence images, acquired with the 100× objective, a portion of a field of erythrocytes suspended in BSA-containing solution A and allowed to settle on a cover glass for parfocal imaging. The images show that the cells loaded with high levels of fura-2 retained their biconcave shape. At the Ca^{2+}-free fura-2 excitation wavelength (380 nm) the extinction coefficient of HbO_2 is about 25 mM(heme)$^{-1}$ cm^{-1}. For a red cell with a maximum thickness of about 2 μm, and an Hb (tetrameric) molarity [Hb] of about 5 mM, the maximum absorption at 380 nm is approx. $2 \cdot 10^{-4} \times 25 \times 4 \times 5 = 0.10$. The attenuation of the exciting light within the cell is therefore negligible, and if fura-2 is uniformly distributed in the cytoplasm, its fluorescence intensity recorded at a particular pixel is approximately

$$I_F = (\text{constant}) I_{ex} \Phi [\text{Fu}] x \quad (1)$$

where I_{ex} is the light-intensity of the excitation beam, Φ is the fluorescence quantum yield of fura-2, [Fu] is its molarity in the cell, and x is the thickness of the cell at the pixel in question. If the red cell were examined by collimated light, its transmission intensity image would be given by

$$I_T = I_0 10^{-\epsilon[\text{Hb}]x} \quad (2)$$

so that

$$\log(I_0 / I_T) = \epsilon [\text{Hb}] x \quad (3)$$

where I_0 and I_T are the incident and transmitted intensities, respectively, and ϵ is the molar extinction coefficient of hemoglobin at 415 nm. Therefore, if both Hb and fura-2 are distributed uniformly within the cell, the I_F and $\log(I_0/I_T)$ profile images have the same shapes according to Eqns. 1 and 3. Comparison of the smoothed I_F (Fig. 2a) and $\log(I_0/I_T)$ (Fig. 2b) profiles for three typical fura-2-loaded red cells shows that the two profiles indeed have similar shapes. Since the transmission and fluorescence images in the present study were obtained using objective and condenser lenses with high numerical apertures, only an approximate agreement with Eqns. 1 and 3 can be expected.

In order to obtain statistically valid data on the distribution of fluorescence intensities emitted by individual cells, approx. 1000 cells were imaged in both the transmission and fluorescence modes at lower magnification, using a 40× objective; a typical pair of such images is shown in Fig. 3. In Fig. 4, histograms of data obtained in this way show that the distribution of fluorescence intensities emitted by individual cells has a width at half maximum of approx. 20% of its mean. The fura-2 fluorescence intensities emitted by most red cells are within a factor of about two; cells at the extreme of the range differ by a factor of less than four.

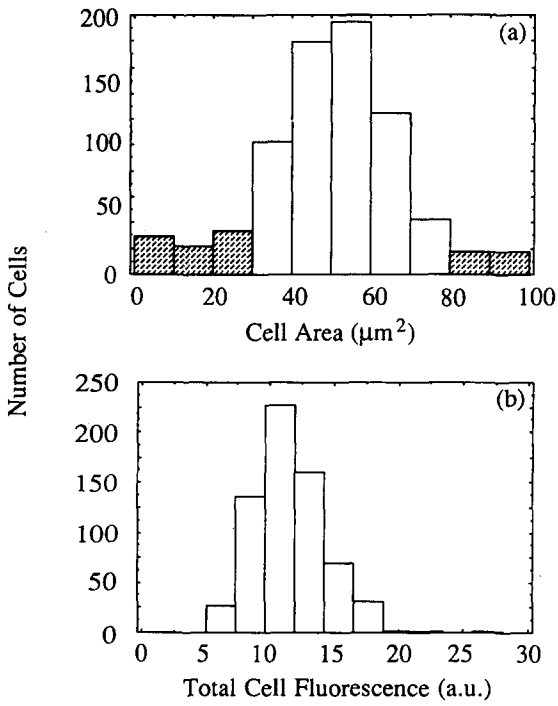

Fig. 4. Histograms showing the distribution of cell areas (a) and of total cell fluorescence emitted by fura-2-loaded red cells (b). (a) The distribution of areas (in μm^2) was determined for fura-2-loaded red cells from their transmission images (at 415 nm, cf., Fig. 3). The cells with areas of less than 30 and greater than 80 μm^2 (shown stippled in the histogram) were excluded from the cytometric analysis; they account for 12% of the total and represent edge-on cells and unresolved multiple cells, respectively. The average diameter of the remaining cells is 8.1 μm. (b) The total fluorescence of each cell, in arbitrary units (a.u.), was calculated by integrating the fura-2 fluorescence intensity (recorded by its fluorescence image) over the cells' area (determined from its transmission image).

Conclusions

Quantitative fluorescence imaging of fura-2 incorporated in intact red cells demonstrates that the chelator was loaded with considerable homogeneity among the cells and within each cell. This validates assumptions made previously in experiments with non-fluorescent incorporated Ca^{2+} chelators, which helped characterize important aspects of Ca^{2+} transport and turnover in normal and abnormal red cells [1,6,15]. It is shown

that neither the loading nor the presence of the high concentrations of fura-2 required to overcome quenching by hemoglobin affect the red cells' integrity or shape, when they are suspended in plasma with normal Ca^{2+} or with Ca^{2+} reduced by excess EGTA. These results demonstrate the feasibility of fura-2 and Ca^{2+} imaging of intact red cells, despite considerable quenching of probe fluorescence by hemoglobin.

Acknowledgements

This work was supported by the Wellcome Trust (UK) and by NIH grants 1R24-RR05272, HL21016 and HL28018.

References

1 Lew, V.L., Tsien, R.Y., Miner, C. and Bookchin, R.M. (1982) Nature 298, 478–481.
2 Bookchin, R.M., Lew, V.L., Nagel, R.L. and Raventos, C. (1981) J. Physiol. 312, 65P.
3 Bookchin, R.M. and Lew, V.L. (1978) J. Physiol. 284, 93P.
4 Lew, V.L., Hockaday, A., Sepulveda, M.I., Somlyo, A.P., Somlyo, A.V., Ortiz, O.E. and Bookchin, R.M. (1985) Nature 315, 586–589.
5 Ortiz, O.E., Lew, V.L. and Bookchin, R.M. (1986) Blood 67, 710–715.
6 Bookchin, R.M., Ortiz, O.E., Shalev, O., Tsurel, S., Rachmilewitz, E.A., Hockaday, A. and Lew, V.L. (1988) Blood 72, 1602–1607.
7 Tsien, R.Y. (1981) Nature 290, 527–528.
8 Lew, V.L. and García-Sancho, J. (1989) Methods Enzymol. 173, 100–112.
9 Tiffert, T., García-Sancho, J. and Lew, V.L. (1984) Biochim. Biophys. Acta 773, 143–156.
10 Orringer, E.P. and Mattern, W.D. (1976) N. Engl. J. Med. 294, 1416–1420.
11 García-Sancho, J. (1985) Biochim. Biophys. Acta 813, 148–150.
12 Sassaroli, M., DaCosta, R., Väänänen, H. and Eisinger, J. (1993) J. Lab. Clin. Med. 121, in press.
13 Sassaroli, M., DaCosta, R., Väänänen, H. and Eisinger, J. (1992) Cytometry 13, 339–345.
14 Tsien, R.Y., Rink, T.J. and Poenie, M. (1985) Cell Calcium 6, 145–157.
15 Bookchin, R.M., Ortiz, O.E. and Lew, V.L. (1991) J. Clin. Invest. 87, 113–124.